El-Sayed, S., et al., 2021, Diverse marine fish assemblages inhabited the paleotropics during the Paleocene-Eocene thermal maximum: Geology, v. 49, https://doi.org/10.1130/G48549.1

Supplemental material to

Diverse marine fish assemblages inhabited the paleotropics during the Paleocene-Eocene thermal maximum

Sanaa El-Sayed[1]*, Matt Friedman[2], Tarek Anan[3], Mahmoud A. Faris[4], Hesham Sallam[1,5]

[1]*Mansoura University Vertebrate Paleontology Center (MUVP), Department of Geology, Faculty of Science, Mansoura University, Mansoura 35516, Egypt*

[2]*Museum of Paleontology, Department of Earth and Environmental Sciences, University of Michigan, 1105 N University Ave, Ann Arbor, MI 48103, USA*

[3]*Department of Geology, Faculty of Science, Mansoura University, Mansoura 35516, Egypt*

[4]*Department of Geology, Faculty of Science, Tanta University, Tanta 31512, Egypt*

[5]*Institute of Global Health and Human Ecology (I-GHHE) School of Sciences and Engineering American University in Cairo AUC Avenue, PO Box 74 New Cairo 11835, Egypt*

SUPPLEMENTAL METHODS

Details of Ras Gharib A

The Ras Gharib A site is located in the Eastern Desert of Egypt, approximately 85 km to the west of the city of Ras Gharib on the coast of the Gulf of Suez (28º 15′N, 32º 13′E; Fig. 1). This locality exposes sedimentary rocks ranging in age from Late Cretaceous to Eocene (Fig. S1A). Stratigraphic sections for Ras Gharib A were created (Figs 2, S2) and lithological samples were collected for the study of calcareous nannofossils (Tables S1-S3). Fish specimens reported here derive from the brown phosphatic shale immediately above the black shale that marks the base of the Dababiya Quarry Member (DQM) of the Esna Shale Formation (Fig. S1B).

Fossil Excavation and Collection

Fossil fishes occur throughout the ~15 cm band of phosphatic shale at the base of the DQM (Fig. 2, Fig. S2), and were collected by quarrying. The most delicate fish specimens, including those preserved across several fragmented blocks, were encased in plaster of Paris *in situ* and cut out of the rock. Most fossils needed minimal preparation. Overlying sediment was removed from larger, more stable specimens using pin vises under a microscope. All specimens are curated at the Mansoura University Vertebrate Paleontology center (MUVP), Mansoura University, Egypt, in accordance with provincial laws.

Biostratigraphic Approach

Standard smear slides were prepared for the study of calcareous nannoplankton following the method described by Perch-Nielsen (1985) and Bown and Young (1998). These were studied with a polarizing microscope (Tanta University) at magnification of x1250, using bright field and cross-polarized light. Some of the stratigraphically important nannofossil species were photographed (Fig. S2). We used the Paleogene nannofossil zone (NP) of Martini (1971), the Paleogene nannofossil zone (CP) of Okada and Bukry (1980), and the Paleocene calcareous nannofossil zone (CNP) and the Eocene calcareous nannofossil zone (CNP) of Agnini et al (2014) for the upper Paleocene-lower Eocene interval (Table S2).

Faunal Analysis

In order to place the Ras Gharib A fauna in the broader context of Late Cretaceous and early Paleogene fish assemblages, we undertook quantitative comparison of the composition of marine faunas of this age. We considered the following body-fossil (rather than otolith) faunas based on available literature:

> <u>Latest Campanian-earliest Maastrichtian</u>: Salento limestone, Nardò, Italy (Belmonte et al., 2016).

Maastrichtian: Ciply Malogne Phosphatic Chalk Formation, Belgium (Friedman, 2012); Maastricht Formation, the Netherlands (Friedman, 2012); Pindos Unit, Eurytania, Greece (Argyriou and Davesne, 2021).

Danian: Copenhagen Limestone Formation, Limhamn Quarry, Sweden (Davis, 1890; Adolfssen et al., 2017); Tenejapa and Lacandón formations, Palenque, Mexico (Alvarado-Ortega et al., 2015; Cantalice and Alvarado-Ortega, 2016; Cantalice et al. 2018, 2020).

Selandian: Lanada Section (Layer 5), Cabinda Enclave, Angola (Solé et al., 2019).

PETM: Dababiya Quarry Member, Ras Gharib A, Egypt (this study); Danata Formation, Uilya-Kushlyuk, Turkmenistan (Bannikov and Parin, 1997; Bannikov, 2000); Stolleklint Clay, Denmark (Bonde, 1997 Bonde et al., 2008); Kheu River, Kabardino-Balkaria (Bannikov and Carnevale, 2012; Bannikov et al., 2017).

Ypresian: "Nummulitic Limestone," Bolca, Italy (Carnevale et al., 2014; Davesne et al., 2016; Marramà et al., 2019, 2020); Monte Solane, Italy (Giusberti et al., 2014); London Clay Formation, United Kingdom (Friedman et al., 2016); Fur Formation, Fur, Denmark (Bonde, 1997; Bonde et al., 2008); Kapurdi Formation, Rajasthan, India (Sanhi and Choudhary, 1972; Bannikov and Tyler, 1994; Friedman and Johnson, 2005; Forey and Hilton, 2010); *Cucullaea* I Allomember, La Meseta Formation, Seymour Island, Antarctica (Reguero et al., 2012).

Lutetian: Calcaire Grossier, Paris Basin, France (Priem, 1908; Gaudant, 1979; Merle, 2008); Lillebaelt Clay, Denmark (Schwarzhans, 2007; Bonde et al., 2008); Dabakhan Canyon, Georgia (Bannikov and Parin, 1997).

Bartonian: Gorny Luch, North Caucasus (Bannikov and Parin, 1997; Bannikov and Tyler, 2001, 2006, 2008; Bannikov, 2002, 2004a, b; Prokofiev and Bannikov, 2002; Bannikov et al., 2011).

?Priabonian: Pabdeh Formaton, Elam, Iran; Istehbanât, Iran (Arambourg, 1967).

Taxonomic conventions. We assembled faunal lists based on overviews of particular assemblages augmented with subsequent papers describing additional taxa. In rare cases, we re-assigned taxa to other families based on subsequent studies or our own observations of fossil material. For the latter case, we emphasize the so-called 'veliferoid' lampidiforms. Here we regard †*Turkmene* and †*Whitephippus* as members of Lampridae, †*Bathysoma* and †*Palaeocentrotus* as members of †Palaeocentrotidae (Bannikov, 2014), and †*Danatina* and various †*Analectis*-like taxa as members of an unnamed group we informally term 'analectids.'

Level of taxonomic comparison. Data were compiled at the family level where possible, reflecting the fact that the vast majority of genera are restricted to specific localities. We did make limited use of more inclusive groups. This reflected cases where fossil specimens clearly belong to clades including multiple families, but are either: (1) placed in monotypic families restricted to single localities, or (2) are of uncertain familial placement. To accommodate such instances, we used the following suprafamilial clades in our compendium in lieu of their constituent families:

Gadiformes minus Bregmacerotidae; Xiphioidei (excluding †Palaeorhynchidae), Stromateoidei, Trichiuroidei, Clupeoidei, Engrauloidei, Ellimmichthyiformes, Anguilloidei, and Zeiformes. We also used suprafamilial clades in two additional lineages: Tetraodontiformes and Syngnathiformes. For tetraodontiforms, we recognize the following groups based on the total-evidence phylogeny presented by Arcila and Tyler (2017): Triacanthoidea (Triacanthidae, Triacanthodidae, †Moclaybalistidae), Ostracioidea (†Spinacanthidae, †Protobalistidae, Ostraciidae, Aracanidae), Balistoidea (Balistidae, Monocanthidae, †Bolcabalistidae, †Eospinidae), Triodontoidea (†*Ctenoplectus*, Triodon), Moloidea (†Zignoichthyidae, Molidae), Tetraodontoidea (†Balkariidae, Tetraodontidae, Diodontidae). This leaves only one monotypic tetraodontiform group in our compendium: †Eoplectidae, which branches from the gymnodont stem. For syngnathiforms, we recognize the groups Centriscoidea (Centriscidae, Macroramphosidae, †*Gasterorhamphosus*, †Gerpegezhidae) and Aulostomoidea (Solenostomidae, †Eekaulostomidae, Fistulariidae, Aulostomidae, Syngnathidae). The Eocene †Aulorhamphidae is *incertae sedis* among these lineages and we include it as its own clade in our faunal compendium.

Analysis of faunal data. Several metrics are available for comparing the similarities of assemblages based on taxonomic presence/absence data, and their relative merits have been extensively debated in the literature (e.g., Koleff et al., 2003). Issues like unequal sample sizes and variable sampling intensity are often exacerbated for paleontological datasets. Alroy (2015a, b) has shown that a modification of the Forbes index (Forbes, 1907) is relatively robust to the kinds of sampling issues known to afflict presence/absence data in paleontology. We used the R script for calculating the Forbes index provided by Brocklehurst et al. (2018) to determine pairwise distances between all of our assemblages. To determine the number of distinct clusters in our faunal data, we used the average silhouette width criterion for dissimilarity data using the `pamk()` function in the R package `fpc` (Hennig, 2020). We performed both non-metric multidimensional scaling (NMDS) using the `metaMDS()` function in the R package `vegan` (Oksanen et al., 2020) and classic multidimensional scaling (i.e., principal coordinates analysis) using the function `pcoa()` in the `ape` package using the `correction = "lingoes"` option to implement the Lingoes (1971) procedure for yielding results without negative eigenvalues. This permitted visualization of the similarities among assemblages. We found that an NMDS implementing two axes had an acceptable level of stress (~0.17), and also visualized our results from classical scaling on two axes. Ordinations are visualized in Fig. 4 and Supplemental Fig. 7.

Faunal data, an associated R script, and a distance matrix for all assemblages are provided as separate files in Supplemental Material.

SUPPLEMENTAL RESULTS

Calcareous Nannofossil Biostratigraphy of Ras Gharib A

Preservation of the diverse Paleocene-Eocene calcareous nannofossil assemblage of Ras Gharib A varies from moderate to good, except for a dissolution interval devoid of nannofossils that spans the lowermost samples (E31 to E35) of the Dababyia Quarry Member. Recognized nannofossil biozones noted for the section are briefly discussed from base to top. Abbreviations: FO = first occurrence, and LO = last occurrence. In the present study, two nannofossil biozones were identified, and arranged from base to top.

1. *Discoaster mohleri – Heliolithus riedelii* interval Zone (NP7-8). This zone is defined as the stratigraphic interval from the FO of *D. mohleri* to the FO of *D. multiradiatus*. Romein (1979) introduced the *D. mohleri* Zone to include the interval spanning the *D. mohleri* and *H. riedelii* zones of Bramlette and Sullivan (1961) because *H. riedelii* is rare and/or difficult to identify. The contact between zones NP 7-8 and NP9 coincides with the Tarawan/Esna formational contact, with Zone NP7-8 restricted to the Tarawan Formation**.**

2. *Discoaster multiradiatus* Zone (NP9). Martini (1971) used the appearance of *Marthasterites bramlettei* (*Tribrachiatus bramlettei*) to define Top Zone NP9, whereas Okada and Bukry (1980) used the appearance of both *Campylosphaera eodela* and *Rhomboaster* spp. to define Top Subzone CP8a.The disappearance of *Fasciculithus richardii* was used to define Top Zone CNP11 (upper Paleocene; Agnini et al., 2014).

Some authors consider *Tribrachiatus bramlettei* and *Rhomboaster cuspis* as synonyms (e.g., Von Salis et al., 2000). According this view, the bases of Zone NP10 and Subzone NP9b are coincident. On the other hand, other authors believe that the structures of *T. bramlettei* and *Rhomboaster* species are different (e.g., Wei and Zhong, 1996; Raffi et al., 2005; Agnini et al., 2007a, 2007b). The latter concept is followed in our study.

In the present study, the NP9 Zone spans the interval from the first occurrence (FO) of *Discoaster multiradiatus* to the first occurrence (FO) of *Tribrachiatus bramlettei*. The *D. multiradiatus* Zone is equivalent to Zone NP9 of Martini (1971), Subzone CN8a of Okada and Bukry (1980), and CNP11 of Agnini et al. (2014).

A subdivision of Zone NP9 has been suggested by various authors based on the FO of *Campylosphaera dela* or the FOs of *Rhomboaster* spp. and *Discoaster araneus*. In the present study, two biozones were identified: NP9a, and NP9b.

> **NP9a Subzone (upper Paleocene).** This subzone represents the interval between the FO of *Discoaster multiradiatus* to the FOs of *Rhomboaste*r spp., and *Discoaster araneus*. The NP9a Subzone spans the stratigraphic interval of El Hanadi Member at the Ras Gharib A. This subzone is characterized by the dominance of the typical Paleocene species of *Fasciculithus*. *Fasciculithus tympaniformis*, *F. involutus*. *Fasciculithus alanii*, is restricted to Zone NP9a, disappears directly below the P/E boundary (e.g., Dupuis et al., 2003; Faris and Abdel Sabour, 2020). At Ras Garib A, *F. alanii* persists across the Paleocene/Eocene boundary. Consequently, its LO cannot be used as a reliable marker to approximate the NP9a/NP9b zonal boundary. However, *Toweius* spp*., Coccolithus pelagicus*, and *Ericsonia*

subpertusa and *Ericsonia robusta* represent common species among the Paleocene nannofossil assemblages in the NP9a Subzone.

NP9b Subzone (lower Eocene). The base of Subzone NP9b defines the base of the Eocene at the GSSP at the Dababiya Quarry section (Aubry et al., 2007). Several Egyptian and Tethyan sections are marked by the presence of a thin dissolution interval (e.g., Tantawy, 1998, 2006; Dupuis et al., 2003; Youssef, 2015, 2016). A thin dissolution interval (7 cm) is observed in the middle part of Zone NP9 (Beds E-31 to E-35) of the Dababyia Quarry Member at Ras Gharib A, and it is marked by absence of calcareous nannofossils. Based only on calcareous nannofossil biostratigraphy and without stable isotope data, the P/E boundary cannot accurately be located. The lower part of this 7 cm interval may be upper Paleocene in age. There is a lithologic break between the El Hanadi Member (dark gray shale) and Dababiya Quarry Member (black shale with organic matter) that may suggest the presence of minor hiatus at the Paleocene/Eocene interval at Ras Gharib A. In the study section, the NP9b Subzone is marked by the first occurrences and dominance of typical Eocene species of *Discoaster araneus*, and *Rhomboaster cuspis*, *R.spineus*, *Discoaster anartios*, *D. mahmoudii*, and *D. paelikei*, have their first appearances in the upper part of the Dababiya Quarry Member (upper Subzone NP9b). The first occurrence of *Coccolithus bownii* is simultaneous with that of *D. araneus* and species of *Rhomboaster* (*R. cuspis*, *R. bitrifida*), and occur at the base of Subzone NP9b of the study section (sample E-36). This zone is also characterized by high abundance of *Neochiastozygus junctus*. The first occurrence of *Coccolithus bownii* is simultaneous with the first occurrence of *D. araneus* and *Rhomboaster* spp at the base of Subzone NP9b at the El Aguz and Darb Gaga sections (Kharga-Baris oases; Metwaly and Mahfouz, 2018). *D. mahmoudii* first appears in upper part of Subzone NP9b and disappears within Subzone NP10a in Wadi Matulla section of west central Sinai, Egypt (Abu Shama et al., 2007).

3. *Tribrachiatus contortus* Zone (NP10). This biostratigraphic interval is defined by the FO of *Tribrachiatus bramlettei* at its base and the LO of *Tribrachiatus contortus* at its top. Subzone NP10a spans the interval between the FO of *Tribrachiatus bramlettei* and the FO of *T. digitalis*. Only the basal part of this zone (Subzone NP10a) was distinguished in the study section. It occupies the topmost part of the Dababiya Quarry Member (samples E49 through E54), as well as the entirety of the El Mahmiya Member (samples E-55 through E65). The NP10a of the study section corresponds to the lower part of CP8a of Okada and Bukry (1980) and lower CNE1 of Agnini et al. (2014). The late Paleocene to early Eocene biozones and bioevents are those according to the standard biozonations of Martini (1971; NP), Okada and Bukry (1980; CN), and Agnini et al. (2014; CNP to CNE). The zonal scheme of the present study is shown in Supplemental Table 1.

Overview of nannofossils at Ras Gharib A. Nannofossils are abundant to few, preservation varies from good to moderate throughout the Paleocene-Eocene interval, and diversity is generally high. The Tarawan Chalk covers with Zone NP7/8. The El Hanadi Member (sample E1- E29/30) belongs to Subzone NP9a, and is characterized by the co-occurrence of *Discoaster multiradiatus*, *D. lenticularius*, *D. falcatus*, *D. mohleri*, *Ellipsolithus macellus*, *Ericsonia subpertusa*, *Fasciculithus alanii*, *F. lilianae*, *F. tympaniformis*, *S. primus*, *Ch. consuetus*, *Toweius pertusus*, and others. A majority of the Dababiya Quarry Member (samples E36-E48) belongs to Subzone NP9b. It contains the so-called *Rhomboaster* spp.-*Discoaster araneus* assemblage (RD) that can easily be correlated with the carbon isotope excursion indicative of the onset of the PETM (Dupuis et al. 2003; Aubry et al. 2007). The RD assemblage is indicative of the NP9a/b subzonal boundary (Paleocene/Eocene boundary).

In the present study, the base of the Eocene was placed at the base of the Dababiya Quarry Member in coincidence with the base of Subzone NP9b, which is coincident with the FOs of *Rhomboaster bitrifidia, R cuspis,* and *Discoaster araneus*, The Paleocene/Eocene boundary is delineated at the bases of NP10 (Martini, 1971), CP8b (Okada Bukry, 1980), and CNE1 (Agnini et al., 2014).Other stratigraphic marker species (e.g., *Rhomboaster calcitripa*, *Discoaster anartios*) appear in higher horizons of the study interval.

As a result of the complete absence of nannofossils in the basal part of the Dababyia Quarry Member (dissolution interval, sample E31 to E35) more detailed studies (paleontological, stratigraphical, stable isotopic) are required to confirm the presence or absence of a minor hiatus at the Paleocene/Eocene boundary at Ras Gharib A.

Calcareous nannoplankton from the Paleocene/Eocene boundary interval at Ras Gharib A suggest extreme warming with increased oligotrophy. Evidence includes the sudden first occurrences of excursion nannofossils (*Rhomboaster* spp.-*Discoaster araneus* assemblage), abrupt increase of the warm-water species C. *bownii* (Bown and Pearson, 2009; Self-Trail et al., 2012), and the high abundance of *C. pelagicus* and *Ericsonia subpertusa*.

Conclusions

The biostratigraphic analyses of calcareous nannofossils from the Tarawan and Esna formations at the Ras Gharib A allowed us to recognize the *Discoaster mohleri-Heliolithus reidelii* Zone (NP7/8) in the upper Tarawan Formation. The *Discoaster multiradiatus* Zone divided into subzones NP9a of upper Paleocene age and NP9b of lower Eocene age, and covers the El Hanadi Member and the lower part of the Dababiya Quarry Member of the Esna Formation. The NP10a Subzone spans the upper part of the Dababiya Quarry Member and the overlying El Mahmiya Member. At the Ras Gharib A, the lowermost samples (E31 to E35, 7 cm thick), representing the basal part of the Dababyia Quarry Member (dissolution interval) and is barren of calcareous nannofossils. This dissolution interval was previously recorded in numerous sections in Egypt (e.g., Khozyem et al., 2013; Youssef, 2015, 2016; Faris and Abdel Sabour, 2020).

The lower Eocene is placed within the basal part of the Dababyia Quarry Member. The P/E boundary is delineated by the first occurrences of the *Rhomboaster* spp.-*Discoaster araneus* (RD) assemblage. *R. spineus*, *Discoaster anartios*, *D. mahmoudii*, and *D. paelikei* first appear within upper part of NP9b of the study interval.

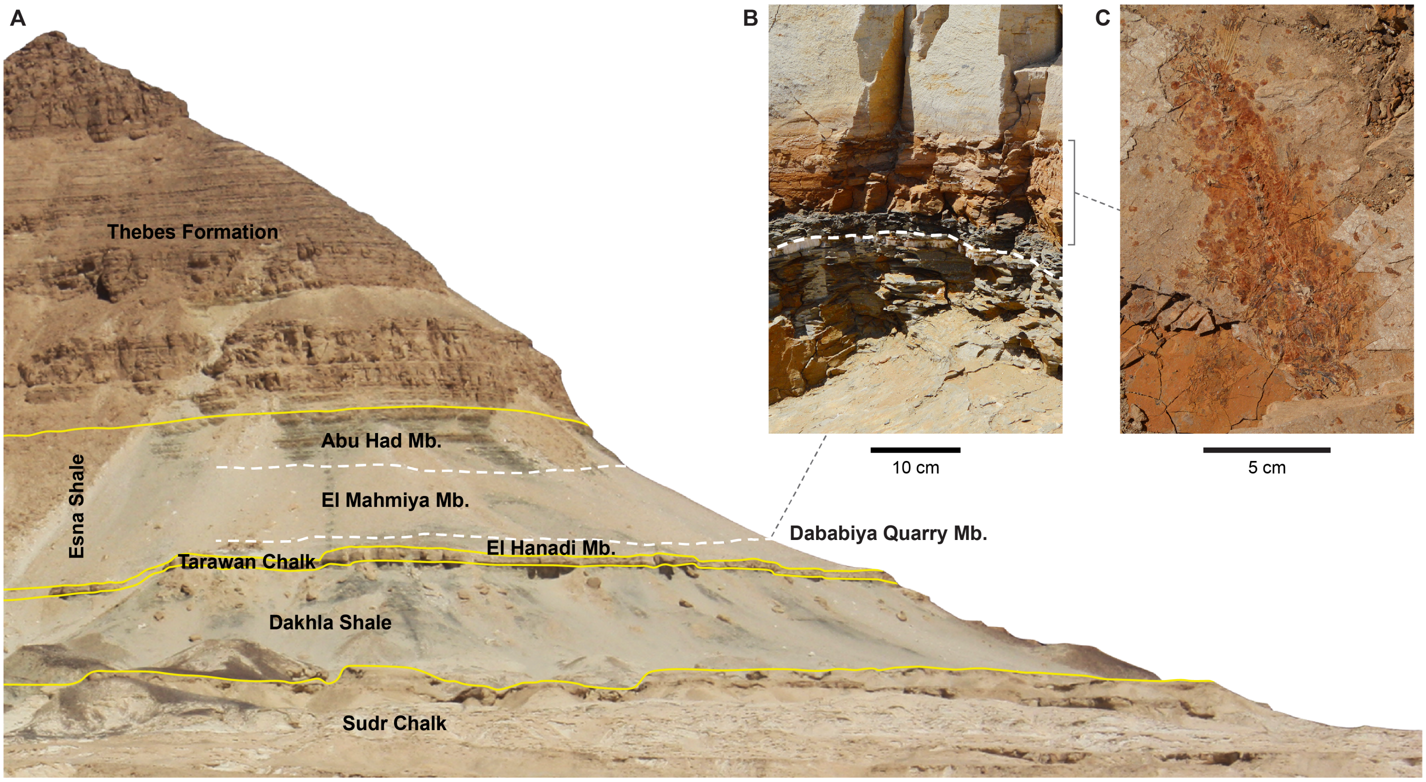

Figure S1. Geological context of Ras Gharib A section, Eastern Desert, Egypt. (A) field photograph of sedimentary sequence at Ras Gharib A, with divisions between principal stratigraphic units marked. (B) close-up view of the Dababiya Quarry Member of the Esna Shale, with white dotted line showing inferred boundary between the Paleocene and Eocene based on regional correlation. (C) field photograph of the fish-bearing layer within the Dababiya Quarry Member, showing fossil remains *in situ*.

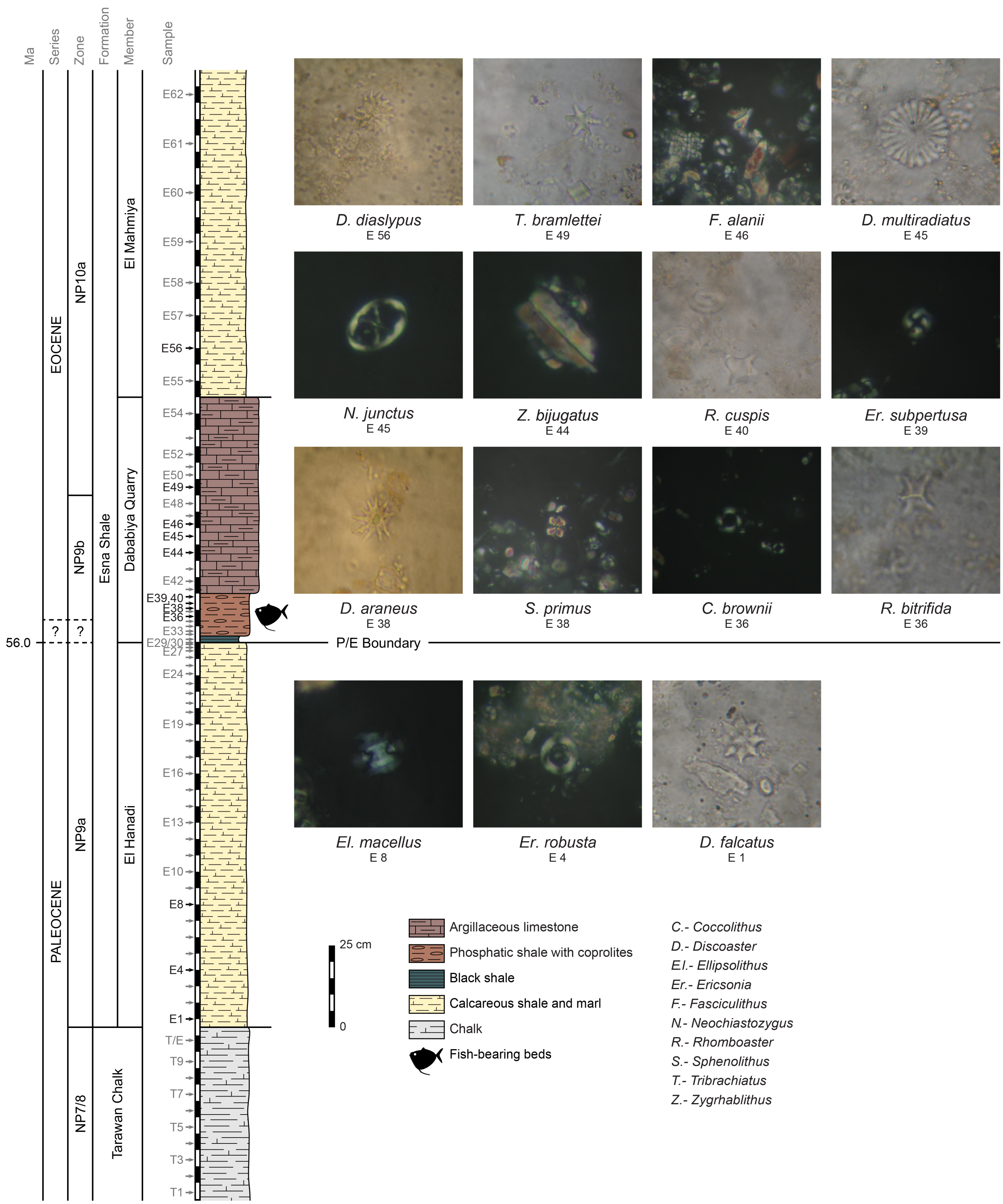

Ma
Series
Zone
Formation
Member
Sample
EOCENE
PALEOCENE
NP10a
NP9b
NP9a
NP7/8
Esna Shale
Tarawan Chalk
El Mahmiya
Dababiya Quarry
El Hanadi
56.0
?
?
P/E Boundary
D. diaslypus
E 56
T. bramlettei
E 49
F. alanii
E 46
D. multiradiatus
E 45
N. junctus
E 45
Z. bijugatus
E 44
R. cuspis
E 40
Er. subpertusa
E 39
D. araneus
E 38
S. primus
E 38
C. brownii
E 36
R. bitrifida
E 36
El. macellus
E 8
Er. robusta
E 4
D. falcatus
E 1
25 cm
0
Argillaceous limestone
Phosphatic shale with coprolites
Black shale
Calcareous shale and marl
Chalk
Fish-bearing beds
C.- Coccolithus
D.- Discoaster
El.- Ellipsolithus
Er.- Ericsonia
F.- Fasciculithus
N.- Neochiastozygus
R.- Rhomboaster
S.- Sphenolithus
T.- Tribrachiatus
Z.- Zygrhablithus

Figure S2 (previous page). Measured stratigraphic section of Ras Gharib A section, Eastern Desert, Egypt. Stratigraphic column shows lithostratigraphy of the Tarawan Chalk and the Esna Shale formations. Numbers to the left of the straigraphic column indicate sampling intervals for microfossils. Samples in black text correspond to index calcareous nannoplankton fossils recovered from the Esna Shale shown in individual photographs to the right.

Table S1. Detailed lithostratigraphic description of Ras Gharib A section, Eastern Desert, Egypt. Samples were taken from the middle of the indicated thickness.

Sample	Description	Thickness (cm)	Calcareous nanoplankton zonation
Esna Shale: El Mahmiya Member			NP10a
E65	Marl: gray, massive, very hard	**15**	
E64	Marl: gray, massive, very hard	**15**	
E63	Marl: gray, massive, very hard	**15**	
E62	Marl: gray, massive, hard	**15**	
E61	Marl: gray, massive, very hard	**15**	
E60	Marl: gray, massive, very hard	**15**	
E59	Shale: gray, massive, calcareous, very hard	**15**	
E58	Shale: gray, massive, calcareous, hard	**10**	
E57	Shale: gray, massive, calcareous, hard	**10**	
E56	Shale: gray, massive, calcareous, hard	**10**	
E55	Shale: gray, massive, calcareous, hard	**10**	
Esna Shale: Dababiya Quarry Member			
E54	Limestone: gray, massive, very hard	**10**	
E53	Limestone: gray, massive, very hard	**5**	
E52	Limestone: gray, massive, very hard	**5**	
E51	Limestone: gray, massive, very hard	**2.5**	
E50	Limestone: gray, massive, very hard	**2.5**	
E49	Limestone: gray, massive, very hard	**5**	
E48	Limestone: gray, massive, very hard	**5**	NP9b
E47	Limestone: gray, massive, hard	**2.5**	
E46	Limestone: gray, massive, hard	**2.5**	
E45	Limestone: light gray, massive, very hard	**5**	
E44	Limestone: light gray, massive, very hard	**5**	
E43	Limestone: light gray, massive, very hard	**5**	
E42	Limestone: light gray, massive, very hard	**2.5**	
E41	Limestone: light gray, massive, very hard	**2.5**	

E40	Shale: light brown, fissile, calcareous, slightly hard	**2**	
E39	Shale: grayish brown, fissile, highly calcareous, slightly hard	**2**	
E38	Shale: grayish brown, fissile, calcareous, slightly hard	**1**	
E37	Shale: light brown, fissile, slightly calcareous, slightly hard	**1**	
E36	Shale: light brown, fissile, phosphatic, calcareous, contains fish remains	**2**	
E35	Shale: dark brown, fissile, phosphatic, contains fish remains	**1**	**?**
E34	Shale: brown, fissile, phosphatic	**2**	
E33	Shale: brown, fissile, phosphatic	**1**	
E32	Shale: brown, fissile, phosphatic, contains fish remains	**1**	
E31	Shale: black, fissile, contains organic matter, gypsiferous	**2**	
E29/30	Shale: black from top and gray from bottom, fissile, moderately hard	negligible	**NP9a**
	Esna Shale: El Hanadi Member		
E29	Shale: dark gray, fissile, hard, contains black laminae	**1**	
E28	Shale: dark gray, contains iron oxides, calcareous	**1**	
E27	Shale: dark gray, fissile, contains black laminae and iron oxides, highly calcareous	**1**	
E26	Shale: dark gray, fissile, slightly hard, highly calcareous, contains iron oxides	**3**	
E25	Shale: gray, very hard, contains iron oxides, calcareous, massive	**2**	
E24	Shale: gray, very hard, contains iron oxides, calcareous, massive	**3**	
E23	Shale: gray, very hard, contains iron oxides, calcareous	**3**	
E22	Marl: gray, very hard, massive, highly calcareous	**3**	
E21	Shale: gray, very hard, massive, calcareous	**3**	
E20	Marl: light gray, very hard, massive	**2.5**	
E19	Marl: light gray, very hard, massive	**5**	
E18	Marl: light gray, very hard, massive	**5**	
E17	Shale: light gray, very hard, massive, calcareous	**5**	
E16	Shale: gray, hard, massive, calcareous, gypsiferous	**5**	
E15	Shale: gray, very hard, massive, calcareous	**5**	

E14	Shale: gray, very hard, massive, calcareous, gypsiferous	**5**	
E13	Shale: gray, hard, massive, slightly calcareous	**5**	
E12	Shale: gray, hard, massive, calcareous	**5**	
E11	Shale: gray, very hard, massive, calcareous	**5**	
E10	Shale: gray, very hard, massive, calcareous	**5**	
E9	Shale: gray, very hard, massive, calcareous	**5**	
E8	Shale: gray, moderately hard, massive, calcareous	**5**	
E7	Marl: gray, very hard, massive	**5**	
E6	Marl: gray, very hard, massive	**5**	
E5	Marl: gray, very hard, massive	**5**	
E4	Shale: gray, hard, massive, calcareous	**5**	
E3	Shale: gray, moderately hard, massive, calcareous	**5**	
E2	Shale: brownish gray, moderately hard, massive, calcareous	**5**	
E1	Shale: gray, moderately hard, massive, calcareous	**5**	
Tarawan Chalk			
T/E	Chalky limestone from bottom and shale from top	**8**	
T9	Chalk: grayish white, very hard	**5**	
T8	Chalk: grayish white, very hard	**5**	
T7	Chalk: grayish white, very hard	**5**	
T6	Chalk: grayish white, very hard	**5**	**NP7/8**
T5	Chalk: grayish white, very hard	**5**	
T4	Chalk: grayish white, very hard	**5**	
T3	Chalk: grayish white, very hard	**5**	
T2	Chalk: grayish white, very hard	**5**	
T1	Chalk: grayish white, very hard	**5**	

Table S2: Late Paleocene to early Eocene biozones and bioevents according to the standard biozonations of Martini (1971) (NP), Okada and Bukry (1980) (CP), Agnini et al. (2014) (CNP to CNE), and the zonal scheme of the present study. First occurrence indicated by horizontal line with downward tick; last occurrence indicated by horizontal line with upward tick. Abbreviations: BZ, base zone; CRZ, concurrent range zone; TZ, top zone.

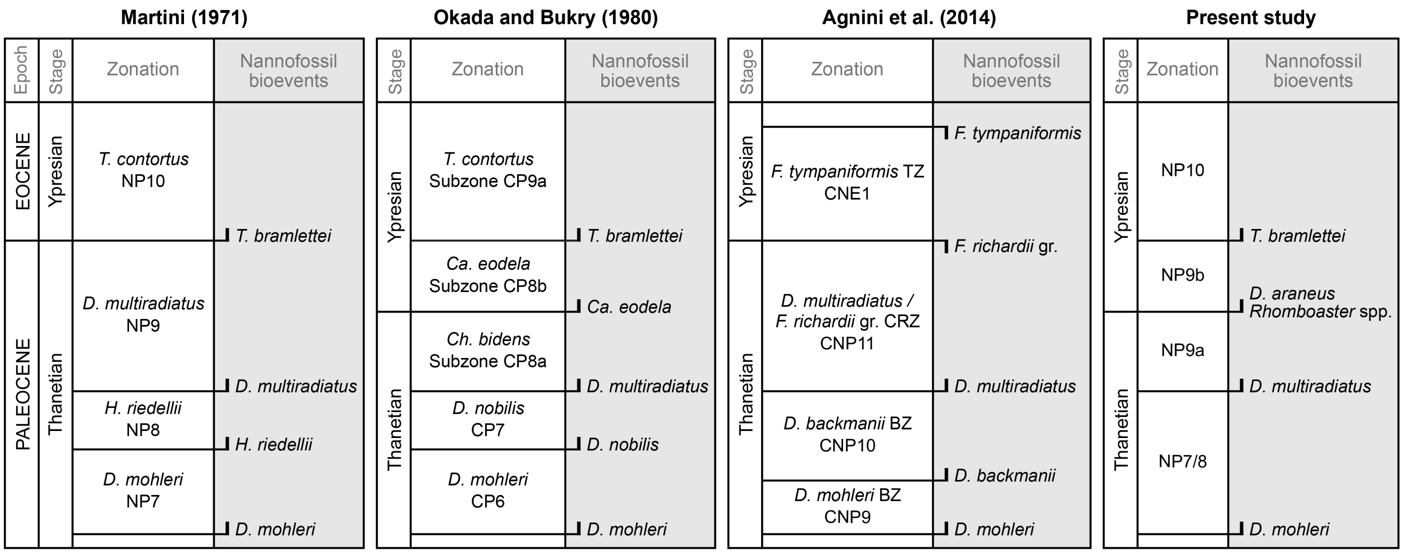

Table S3. Carbonate/sand/mud content from samples taken near the Paleocene/Eocene boundary at Ras Gharib A, Eastern Desert, Egypt.

Rock Unit		Sample	Carb. %	Sand %	Mud %	Name
Esna Shale	DQM	**E36**	64.7	0.0	35.3	Limestone
		E35	15.0	0.0	85.0	Calcareous shale
		E34	7.8	0.1	92.1	Shale
		E33	13.6	0.2	86.2	Calcareous shale
		E32	6.1	1.0	92.9	Shale
		E31	12.7	2.8 gypsum	84.5	Calcareous shale
		E29/30	10.9	0.0	89.1	Shale
	El Hanadi Mb	**E29**	33.8	0.0	66.2	Calcareous shale
		E28	39.7	0.0	60.3	Calcareous shale
		E27	29.1	0.0	70.9	Calcareous shale

FISH FAUNA FROM RAS GHARIB A

Nearly 290 fish fossils were collected during the course of three field trips in 2017, 2018, and 2019 (Table S4). Fish fossils occur throughout the basal 7 cm of the Dababiya Quarry Member (DQM). These are mostly heavily flattened, but some larger specimens show substantial three-dimensional relief (e.g., osteoglossid vertebrae shown in Fig. 3b). Not all specimens are complete, but most are partially articulated skeletons. Some are incomplete only because they were truncated by natural breaks in the rock. The phosphatic shale layers of the DQM degrades very easily upon exposure to the humid conditions, making specimens difficult to collect intact. As a consequence, many collected specimens can only be assigned to higher-level taxa. We anticipate that future collecting will permit more precise taxonomic identifications.

Actinopterygian fishes collected from the Dababiya Quarry Member at Ras Gharib A are listed below. Counts for some taxa are approximate, and only specimens figured or mentioned in this paper are assigned MUVP catalog numbers; these are indicated by underlined text. All remaining examples are listed by field numbers with the prefix “PETM.”

Osteoglossomorpha: Osteoglossidae (*n* = 5). PETM 18116, PETM 18122-18123, PETM 19174 (MUVP 529; Fig. 3a), PETM 19175 (MUVP 546; Fig. 3b).

Clupeomorpha: Clupeoidei (*n* = 3). PETM 18126, PETM 19176 (MUVP 524c), PETM 19183.

Stomiiformes: Sternoptychidae (*n* = 1). PETM 19177 (MUVP 523d).

Aulopiformes: Paralepididae (*n* = 1). PETM 19178 (MUVP 548e).

Carangaria: Menidae: *Mene* (*n* = 65). PETM 1802, PETM 1804, PETM 1810, PETM 1816, PETM 1821, PETM 1827, PETM 1831, PETM 1842, PETM 1847, PETM 1848, PETM 1881, PETM 1895-1895, PETM 18100, PETM 18114, PETM 18120, PETM 18124, PETM 18128, PETM 1833, PETM 1958, PETM 1964-1965, PETM 1979-1999, PETM 19100-19116, PETM 19142-19143, PETM 19150, PETM 19172 (MUVP 556g).

Pelagiaria: Trichiuroidei (*n* = 1). PETM 19173 (MUVP 537; Fig. 3f).

Pelagiaria: Scombridae (*n* = 5). PETM 18121, PETM 1909, PETM 1957, PETM 1972, PETM 19174 (MUVP 528; Fig. 3h).

Percomorpha indet. (*n* = 73): PETM 1801-1807, PETM 1814, PETM 1822, PETM 1826, PETM 1828, PETM 1833-1844, PETM 1839, PETM 1850-1851, PETM 1853, PETM 1856-1857, PETM 1860, PETM 1862, PETM 1865, PETM 1869, PETM 1871-1873, PETM 1877-1878, PETM 1880, PETM 1888-1891, PETM 1896-1897, PETM 18102, PETM 18108, PETM 18188, PETM 18125, PETM 18127, PETM 18132, PETM 1901, PETM 1908, PETM 1910, PETM 1912, PETM 1914,

PETM 1920, PETM 1923-1924, PETM 1938, PETM 1939, PETM 1941, PETM 1951, PETM 1954, PETM 1956, PETM 1961, PETM 1963, PETM 1966, PETM 1978, PETM 19137-19139, PETM 19144, PETM 19146, PETM 19157, PETM 19179 (MUVP 526; Fig. 3i), PETM 19180 (MUVP 552; Fig. 3m), PETM 19181 (MUVP 527; Fig. 3n), PETM 19182 (MUVP 525; Fig. 3o), PETM 19183 (MUVP 519; Fig. 3j), PETM 19184 (MUVP 530; Fig. 3l).

Coprolites (*n* = 13; does not include coprolites on blocks containing other material): PETM 1808-1809, PETM 1849, PETM 1868, PETM 1885, PETM 1892, PETM 18130, PETM 1942, PETM 1977, PETM 19163-19166.

Indeterminate fish scales (*n* = 24; does not include isolated scales on blocks containing other material): PETM 1813, PETM 1815, PETM 1817, PETM 1819, PETM 1832, PETM 1836, PETM 1840, PETM 1844-1846, PETM 1854, PETM 1864, PETM 1882, PETM 1887, PETM 18109, PETM 1904, PETM 1916, PETM 1962, PETM 1968-1969, PETM 19167-19170.

Indeterminate skeletal fragments (*n* = 101; does not include skeletal fragments on blocks containing other material): PETM 1811-1812, PETM 1818, PETM 1820, PETM 1823-1825, PETM 1829-1830, PETM 1835, PETM 1837-1838, PETM 1841, PETM 1843, PETM 1852, PETM 1855, PETM 1858-1859, PETM 1861, PETM 1863, PETM 1866-1877, PETM 1870, PETM 1874-1876, PETM 1879, PETM 1883-1884, PETM 1893, PETM 1898-1899, PETM 18101, PETM 18103-18107, PETM 18111-18113, PETM 18115, PETM 18119, PETM 18131, PETM 1902-1903, PETM 1906, PETM 1911, PETM 1915, PETM 1928, PETM 1930, PETM 1932, PETM 1937, PETM 1944-1945, PETM 1950, PETM 1955, PTEM 1959-1960, PETM 1967, PETM 1970-1971, PETM 1973-1976, PETM 19118-19136, PETM 19140-19141, PETM 19145, PETM 19147-19149, PETM 19151-19156, PETM 19158-19159, PETM 19171.

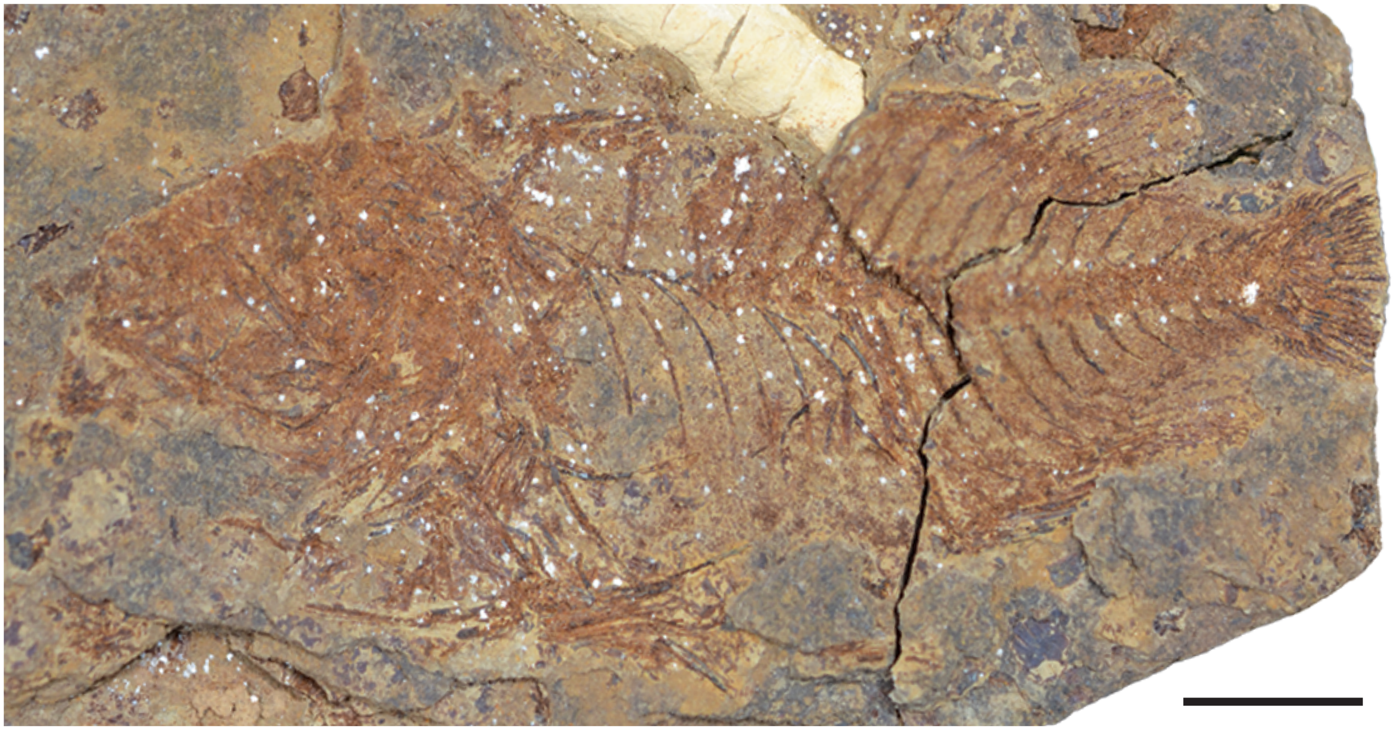

Figure S3. Undetermined percomorph, MUVP 530 (shown in Fig. 3L). Scale equals 5 mm.

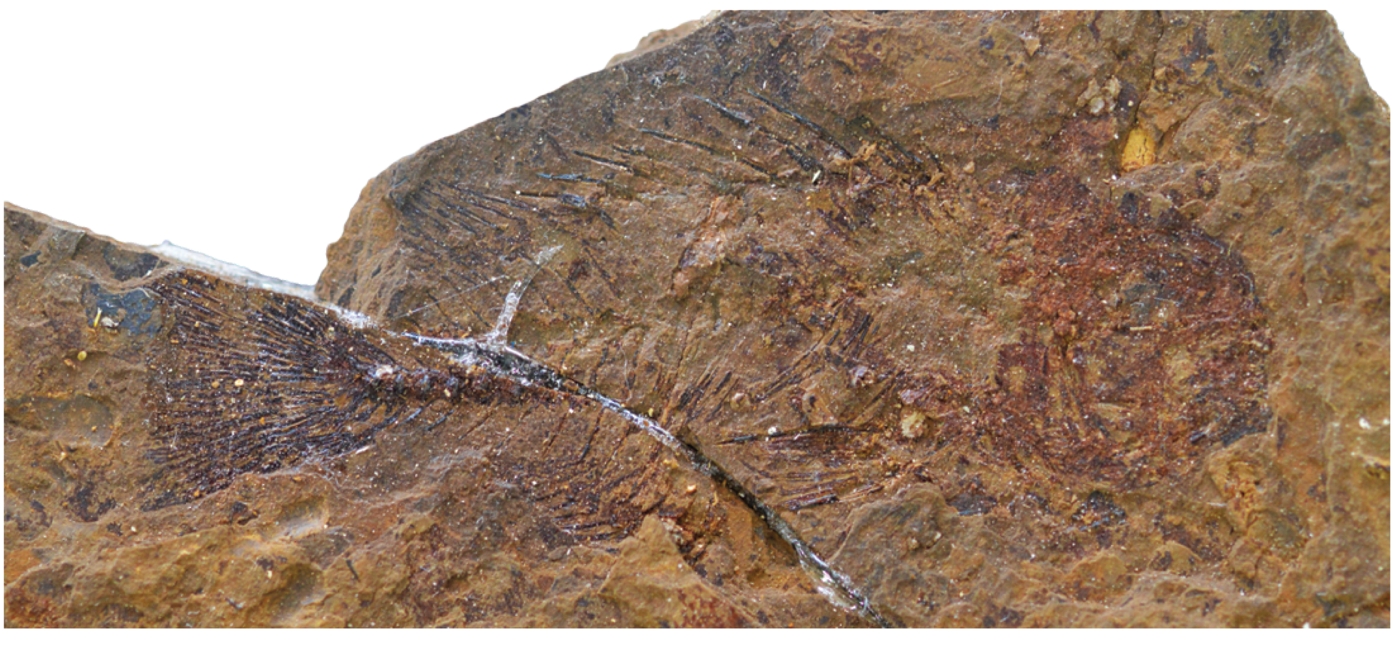

Figure S4. Undetermined percomorph, MUVP 552 (shown in Fig. 3M). Scale equals 10 mm.

Figure S5. Undetermined percomorph, MUVP 527 (shown in Fig. 3N). Scale equals 10 mm.

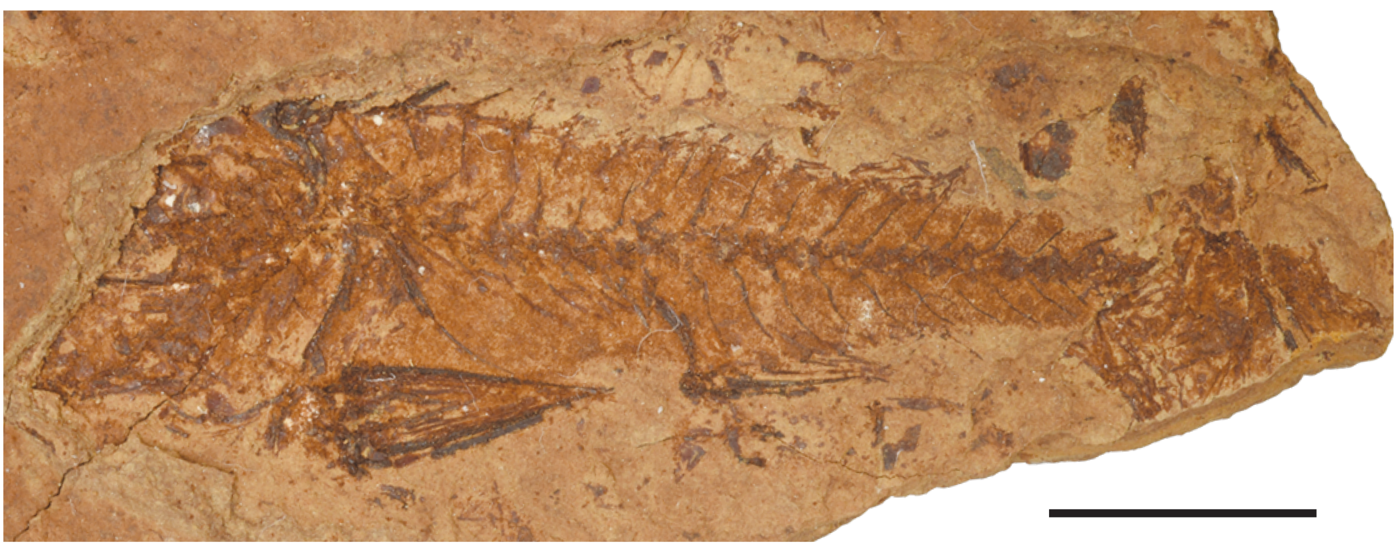

Figure S6. Undetermined percomorph, MUVP 525 (shown in Fig. 3O). Scale equals 5 mm.

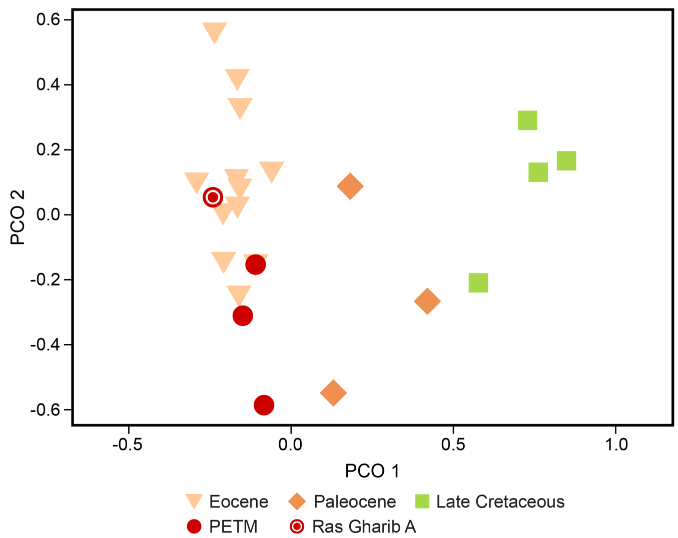

Figure S7. Ordination (metric multidimensional scaling) of pairwise distances of latest Cretaceous-Eocene marine actinopterygian faunas. Similarities measured using Forbes index for presence/absence of families (or more inclusive groups). Ras Gharib A assemblage is indicated with red bull's-eye, and clusters with other faunas from the PETM and Eocene more generally, regardless of paleolatitude. Application of the average silhouette width criterion indicates two clusters: one corresponding to all Eocene (including PETM) faunas and some Paleocene faunas, and another including Late Cretaceous faunas plus the Danian assemblage from the Copenhagen Limestone Formation at Limhamn, Sweden. Numbers in parentheses represent percentage of total variation summarized.

REFERENCES

Abu Shama, A.M., Faris, M., and Al-Wosabi, Kh. A., 2007, Upper Paleocene-Lower Eocene , calcareous nannofossil biostratigraphy of Gebel Matulla section and paleoecology of Gebel Matulla section, southwestern Sinai, Egypt: Proceeding the 5th International Conference of the Geology of Africa, Assiut, Egypt, v. 1, p.33-51.

Adolfssen, J.S., Milàn, J., and Friedman, M., 2017, Review of the Danian vertebrate fauna of southern Scandinavia: Bulletin of the Geological Society of Denmark, v. 65, p. 1-23.

Agnini, C., Fornaciari, E., Raffi, I., Catanzariti, R., Pälike, H., et al., 2014, Biozonation and biochronology of Paleogene calcareous nannofossils from low and middle latitudes: Newsletters on Stratigraphy, Stuttgart, v. 47, p. 131-181.

Agnini, C., Fornaciari, E., Raffi, I., Rio, D., Röhl, U. et al., 2007a, High-resolution nannofossil biochronology of middle Paleocene to early Eocene at ODP Site 1262: implications for calcareous nannoplankton evolution: Marine Micropaleontology, v. 64, p. 215-248.

Agnini, C., Fornaciari, E., Rio, D., Tateo, F., Backman, J. et al., 2007b, Responses of calcareous nannofossil assemblages, mineralogy and geochemistry to the environmental perturbations across the Paleocene/Eocene boundary in the Venetian Pre-Alps: Marine Micropaleontology, v. 63, p. 19-38.

Alroy, J., 2015a, A simple way to improve multivariate analyses of paleoecological data sets: Paleobiology, v. 41, p. 377-386.

Alroy, J., 2015b, A new twist on a very old binary similarity coefficient: Ecology, v. 96, p. 575-586.

Alvarado-Ortega, J., Cuevas-García, M., del Pilar Melgarejo-Damián, M., Cantalice, K.M., Alaniz-Galvan, A., Solano-Templos, G., and Than-Marchese, B.A., 2015, Paleocene fishes from Palenque, Chiapas, southeastern Mexico: Palaeontologia Electronica, v. 18.2.39A, p. 1-21.

Arambourg, C., 1967, Les poissons Oligocènes de l'Iran: Notes et Mémoires sur le Moyen-Orient, v. 8, p. 1-210.

Arcila, D., and Tyler, J.C., 2017, Mass extinction in tetraodontiform fishes linked to the Palaeocene–Eocene thermal maximum: Proceedings of the Royal Society B: Biological Sciences, v. 284, p. 20171771.

Argyriou, T., and Davesne, D., 2021, Offshore marine actinopterygian assemblages from the Maastrichtian-Paleogene of the Pindos Unit in Eurytania, Greece: PeerJ, v. 9, p. e10676.

Aubry, M., Ouda, K., Dupuis, C., Berggren, W.A., Couvering, J.V., Ali, J., Brinkhuis, H., Gingerich, P.R., Heilmann-Clausen, C., Hooker, J., Kent, D.V., King, C., Knox, R., Laga, P., Molina, E., Schmitz, B., Steurbaut, E., and Ward, D., 2007, The Global Standard Stratotype-section and Point (GSSP) for the base of the Eocene Series in the Dababiya section (Egypt): Episodes, v. 30, p. 271-286.

Bannikov, A.F., 2000, New data on late Paleocene marine percoids (Perciformes) of Turkmenistan: Journal of Ichthyology, v. 40, p. 564-570.

Bannikov, A.F., 2002, A new middle-Eocene percoid (Perciformes, Percoidei) from the northern Caucasus: Journal of Ichthyology, v. 42, p. 725-730.

Bannikov, A.F., 2004a, Discovery of a champsodontid (Pisces, Teleostei, Perciformes) in the Eocene of the northern Caucasus: Paleontological Journal, v. 38, p. 311-315.

Bannikov, A.F., 2004b, The first dicovery of an anglerfish (Teleostei, Lophiidae) in the Eocene of the northern Caucasus: Paleontological Journal, v. 38, p. 67-72.

Bannikov, A.F., 2014, A new genus of the family Palaeocentrotidae (Teleostei, Lampridiformes) from the Oligocene of the Northern Caucasus and comments on other fossil Veliferoidei: Paleontological Journal, v. 48, p. 624-632.

Bannikov, A.F., and Carnevale, G., 2012, A long-bodied centriscoid fish from the basal Eocene of Kabardino-Balkaria, northern Caucasus, Russia: Naturwissenschaften, v. 99, p. 379-389.

Bannikov, A.F., Carnevale, G., and Parin, N.V., 2011, The family Caucasichthyidae (Pisces, Perciformes) from the Eocene of the north Caucasus: v. 45, p. 83-89.

Bannikov, A.F., and Parin, N.N., 1997, The list of marine fishes from Cenozoic (Upper Paleocene-Middle Miocene) localities in southern European Russia and adjacent countries: Journal of Ichthyology, v. 37, p. 149-161.

Bannikov, A.F., and Tyler, J.C., 2001, A new species of the luvarid fish genus †*Avitoluvarus* (Acanthuroidei: Perciformes) from the Eocene of the Caucasus in southwest Russia: Proceedings of the Biological Society of Washington, v. 114, p. 579-588.

Bannikov, A.F., and Tyler, J.C., 2004, A revision of the Eocene fish family Exelliidae (Perciformes): Paleontological Journal, v. 28, p. 128-140.

Bannikov, A.F., and Tyler, J.C., 2006, A new species of the genus *Aulorhamphus* (Gasterosteiformes: Aulorhamphidae) from the Eocene of the Caucasus in southwestern Russia: Proceedings of the Biological Society of Washington, v. 119, p. 143-149.

Bannikov, A.F., and Tyler, J.C., 2008, A new genus and species of triggerfish from the middle Eocene of the northern Caucasus, the earliest member of the Balistidae (Tetraodontiformes): Paleontological Journal, v. 42, p. 615-620.

Bannikov, A.F., Tyler, J.C., Arcila, D., and Carnevale, G., 2017, A new family of gymnodont fish (Tetraodontiformes) from the earliest Eocene of the Peri-Tethys (Kabardino-Balkaria, northern Caucasus, Russia): Journal of Systematic Palaeontology, v. 15, p. 129-146.

Belmonte, G., Capasso, L., and Taverne, L.P., 2016, Salento Cretaceous fish in Italian museums and other scientific institutions: Museologica Scientifica, Nouva Serie, v. 10, p. 94-98.

Bonde, N., 1997, A distinct fish fauna from the basal ash series of the Fur/Ølst Formation (U. Paleocene, Denmark): Arhus Geoscience, v. 6, p. 33-48.

Bonde, N., Andersen, S., Niels, H., and Jakobsen, S.L., 2008, Danekræ – Danmarks bedste fossiler: Copenhagen, Glydendal, 224 p.

Bown, P., and Pearson, P., 2009, Calcareous plankton evolution and the Paleocene/Eocene thermal maximum event: new evidence from Tanzania: Marine Micropaleontology, v. 71, p. 60–70.

Bown, P.R., and Young, J.R., 1998, Techniques, *in* Bown, P.R., ed., Calcareous Nannofossil Biostratigraphy: London, UK, Chapman and Kluwer Academic (British Micropalaeontological Society Publications Series), p. 16-28.

Bramlette, M.N., and Sullivan, F.R., 1961, Coccolithophorids and related nannoplankton of the Early Tertiary in California: Micropaleontology, v. 7, p. 129-188.

Brocklehurst, N., Day, M.O., Rubidge, B.S., and Fröbisch, J., 2017, Olson's Extinction and the latitudinal biodiversity gradient of tetrapods in the Permian: Proceedings of the Royal Society, Series B, vol. 284, p. 20170231.

Cantalice, K.M., and Alvarado-Ortega, J., 2015, *Eekaulostomus cuevasae* gen. and sp. nov., an ancient armoured trumpetfish (Aulostomoidea) from Danian (Paleocene) marine deposits of Belisario Domínguez, Chiapas, southeastern Mexico: Palaeontologia Electronica, v. 19.3.53A, p. 1-24.

Cantalice, K.M., Alvarado-Ortega, J., and Alaniz-Galvan, A., 2018, *Paleoserranus lakamhae* gen. et sp. nov., a Paleocene seabass (Perciformes: Serranidae) from Palenque, Chiapas, southeastern Mexico: Journal of South American Earth Sciences, v. 83, p. 137-146.

Cantalice, K.M., Alvarado-Ortega, J., and Bellwood, D.R., 2020, †*Chaychanus gonzalezorum* gen. et sp. nov.: A damselfish fossil (Percomorphaceae; Pomacentridae) from the Early Paleocene outcrop of Chiapas, Mexico: Journal of South American Earth Sciences, v. 98, p. 102322.

Carnevale, G., and Bannikov, A.F., 2015, Pietschellidae fam. nov., a new family of miniature percomorph fishes from the Eocene of Bolca, with the description of a new genus and species: Studi e ricerche sui giaciamenti terziari di Bolca, XVI – Miscellanea Paleontologica, v. 13, p. 17-26.

Carnevale, G., and Bannikov, A.F., 2019, A dragonet (Teleostei, Callionymoidei) from the Eocene of Monte Bolca, Italy: Bollettino della Società Paleontologica Italiana, v. 58, p. 295-307.

Carnevale, G., Bannikov, A.F., Marramà, G., Tyler, J.C., and Zorzin, R., 2014, The Pesciara-Monte Postale *Fossil-Lagerstätte*: 2. Fishes and other vertebrates: Rendiconti della Società Paleontologica Italiana, v. 4, p. 37-63.

Davesne, D., Carnevale, G., and Friedman, M., 2016, *Bajaichthys elegans* from the Eocene of Bolca (Italy) and the overlooked morphological diversity of Zeiformes (Teleostei, Acanthomorpha): Paleontology, v. 60, p. 255-268.

Davis, J.W., 1890, On the fossil fish of the Cretaceous formations of Scandinavia: Scientific Transactions of the Royal Dublin Society, v. 4, p. 363-434.

Dupuis, C., Aubry, M.-P., Steurbaut, E., Berggren, W. A., Ouda, K., Magioncalda, R., Cramer, B.S., Kent, D.V., Speijer, R. P., and Heilmann-Clausen, C., 2003, The Dababiya Quarry Section: Lithostratigraphy, Clay Mineralogy, Geochemistry and Paleontology: Micropaleontology, v. 49, p. 41-59.

Forbes, S.A., 1907, On the local distribution of certain Illinois fishes: an essay in statistical ecology: Bulletin of the Illinois State Laboratory of Natural History, v. 7, p. 272-302.

Giusberti, L., Bannikov, A., Galazzo, F.B., Fornaciari, E., Freiling, J., Luciani, V., Papazzoni, C.A., Roghi, G., Schouten, S., Sluijs, A., Bosellini, F.R., and Zorzin, R., 2014, A new *Fossil-Lagerstäte* from the Lower Eocene of the Lessini Mountains (northern Italy): A multidisciplinary approach: Palaeogeography, Palaeoclimatology, Palaeoecology, v. 403, p. 1-15.

Faris, M., and Abdel Sabour, A., 2020, Late Palaeocene-Early Eocene nannofossil bioevents at Gebel El Aguz, Northern Kharga Oasis, Western Desert, Egypt: Arab Journal Geoscience, v.13, p. 200.

Forey, P.L., and Hilton, E.J., 2010, Two new Tertiary osteoglossid fishes (Teleostei: Osteoglossomorpha) with notes on the history of the family, *in* Elliott, D.K., Maisey, J.G., Yu, X., and Miao, D., eds., Morphology, Phylogeny, and Paleobiogeography of Fossil Fishes: Munich, Germany, Verlag Friedrich Pfeil, p. 215-246.

Friedman, M., 2012, Ray-finned fishes (Osteichthyes, Actinopterygii) from the type Maastrichtian, the Netherlands and Belgium: Scripta Geologica, Special Issue, v. 8, p. 113-142.

Friedman, M., Beckett, H.T., Close, R.A., and Johanson, Z. 2016. English Chalk and London Clay: two remarkable British bony fish *Lagerstätten*: Geological Society of London, Special Publications, v. 430, p. 165-200.

Friedman, M., and Johnson, G.D., 2005, A new species of *Mene* (Perciformes: Menidae) from the Paleocene of South America, with notes on paleoenvironment and a brief review of menid fishes: Journal of Vertebrate Paleontology, v. 25, p. 770-783.

Gaudant, J., 1979, Sur un *Amphistium* (poisson teleosteen, Percoidei) de l'Eocene Parisien: Bulletin d'information des géologues du bassin de Paris, v. 16, p. 11-14.

Hennig, C., 2020, fpc: Flexible Procedures for Clustering. R package version 2.2-9. https://CRAN.R-project.org/package=fpc

Khozyem, H., Adatte, T., Spangenberg, J.E., Tantawy, A.A., and Keller, G., 2013, Palaeoenvironmental and climatic changes during the Palaeocene–Eocene Thermal Maximum (PETM) at the Wadi Nukhul Section, Sinai, Egypt: Journal of the Geological Society of London, v. 170, p. 341-352.

Koleff, P., Gaston, K.J., Lennon, J.J., 2003 Measuring beta diversity for presence-absence data: Journal of Animal Ecology, v. 72, p. 367-382.

Lingoes, J.C., 1971, Some boundary conditions for a monotone analysis of symmetric matrices. *Psychometrika*, v. 36, p. 195–203.

Marramà, G., Bannikov, A.F., and Carnevale, G., 2020, An Eocene scorpionfish from Monte Postale (Bolca Lagerstätte, northeast Italy): Bolletino della Società Paleontologica Italiana, v. 59, p. 105-112.

Marramà, G., Bannikov, A.F., Kriwet, J., and Carnevale, G., 2019, An Eocene paraclupeid fish (Teleostei, Ellimmichthyiformes) from Bolca, Italy: the youngest marine record of double-armoured herrings: Papers in Palaeontology, 5, 83-98.

Martini, E., 1971, Standard Tertiary and Quaternary calcareous nannoplankton Zonation, *in* Farinacci, A., ed., Proceedings of the II Planktonic Conference 2, Rome (1970): Rome, p. 739-785.

Merle, D., 2008, Le contenu paléontologique, *in* Merle, D., ed., Stratotype Lutétien: Paris, Publications Scientifiques du Muséum, 111-227.

Metwally, A.A, and. Mahfouz., K.H., 2018, The Paleocene/Eocene (P/E) boundary along the eastern plateau of Kharga - Baris oases, Western Desert, Egypt: Journal of African Earth Sciences, v.147, p. 569-584.

Okada, H., and Bukry, D., 1980, Supplementary modification and introduction of code numbers to the low-latitude Coccolith Biostratigraphic Zonation (Bukry, 1973, 1975): Marine Micropaleontology, v. 5, p. 321-325.

Oksanen, J., Blanchet, F.G., Friendly, M., Kindt, R., Legendre, P., McGlinn, D., Minchin, P.R., O'Hara, R.B., Simpson, G.L., Solymos, P., Stevens, M.H.M., Szoecs, E., and Wagner, H., 2020, vegan: Community Ecology Package. R package version 2.5-7. https://CRAN.R-project.org/package=vegan

Perch-Nielsen, K., 1985, Cenozoic calcareous nannofossils, *in*, Bolli, H.M., Saunders,J., B., Perch-Nielsen, K., eds., Plankton Stratigraphy: Cambridge, UK, Cambridge University Press, p. 427-554.

Priem, F., 1908, Publications des Annales de Paléontologie: Ètude des poissons fossiles du Bassin Parisien: Paris, Masson et C^ie^, 145 p.

Prokofiev, A.M., and Bannikov, A.F., 2002, A new genus of Stomiiformes (Pisces, Actinopterygii) from the Eocene of the northern Caucasus: Paleontological Journal, v. 36, p. 161-167.

Raffi, I., Backman, J., and Pälike, H., 2005, Changes in calcareous nannofossil assemblage across the Paleocene/Eocene transition from the paleo-equatorial Pacific Ocean. Palaeogeography, Palaeoclimatology, Palaeoecology, v. 226, p. 93-126.

Reguero, M.A., Marenssi, S.A., and Santillana, S.N., 2012, Weddellian marine/coastal vertebrates diversity from a basal horizon (Ypresian, Eocene) of the *Cucullaea* I Allomember, La Meseta Formation, Seymour (Marambio) Island, Antarctica: Peruvian Journal of Biology, v. 19, p. 275-284.

Romein, A.J.T., 1979. Lineages in early Paleogene calcareous nannoplankton: Utrecht Micropaleontology Bulletin, v. 22, p. 1-231.

Sahni, A., and Choudhary, N.K., 1972, Lower Eocene fishes from Barmer, south western Rajasthan, India: Proceedings of the Indian National Science Academy, v. 38A, p. 97-102.

Schwarzhans, W., 1997, Otoliths from casts from the Eocene Lillebælt Clay Formation of Trelde Næs near Fredericia (Denmark), with remarks on the diet of stomatopods: Neues Jahrbuch für Geologie und Paläontologie, Abhandlungen, v. 245, p. 69-81.

Self-Trail, J.M., Powars, D.S., Watkins, D.K., and Wandless, G.A., 2012, Calcareous nannofossil assemblage changes across the Paleocene– Eocene Thermal Maximum: Evidence from a shelf setting: Marine Micropaleontology, v. 92–93, p. 61–80.

Solé, F., Noiret, C., Desmares, D., Adnet, S., Taverne, L., De Putter, T., Mees, F., Yans, J., Steeman, T., Louwye, S., Folie, A., Stevens, N.J., Gunnell, G.F., Baudet, D., Kitambala Yaya, N., and Smith, T., 2019, Reassessment of historical sections from the Paleogene marine margin of the Congo Basin reveals an almost complete absence of Danian deposits: Geoscience Frontiers, v. 10, p. 1039-1063.

Tantawy, A.A., 1998, Stratigraphical and paleoecological studies on some Paleocene-Eocene successions in Egypt: Unpublished Ph.D. Thesis, Assiut University, Egypt, p. 1-273. Tantawy, A.A., 2006, Calcareous nannofossils of the Paleocene-Eocene transition at Qena Region, Central Nile Valley, Egypt: Micropaleontology, v. 52, p. 193-222.

Von Salis, K., Monechi, S., Bybell, L.M., Self-Trail, J., Young, J.R., 2000, Remarks on the calcareous nannofossil genera *Rhomboaster* and *Tribrachiatus* around the Paleocene/Eocene Boundary, *in* Andreasson, F.P., Schmitz, B., and Thompson, E.I., eds., Early Paleogene Warm Climates and Biosphere Dynamics: GFF, p. 138-140

Wei, W., and Zhong, S. 1996. Taxonomy and magnetobiochronology of *Tribrachiatus bramlettei* and *Rhomboaster*: two genera of calcareous nannofossils: Journal of Paleontology, v. 70, p. 7-22.

Youssef, A. 2015. Evaluation of foraminifera and calcareous nannofossils changes across the Late Paleocene/Early Eocene transition at Nag El-Quda section, Upper Nile Valley, Egypt: Geosciences journal, v. 19, p. 641-654.

Youssef, A., 2016, Calcareous nannofossils and paleoenvironments of the Paleocene-Eocene thermal maximum (PETM) interval in central Egypt: Journal of African Earth Sciences, v. 114, p. 203-219.